

Articles

³¹P NMR Probes of Chemical Dynamics: Paramagnetic Relaxation Enhancement of the ¹H and ³¹P NMR Resonances of Methyl Phosphite and Methylethyl Phosphate Anions by Selected Metal Complexes

Jack S. Summers,^{*,†} Charles G. Hoogstraten,[‡] R. David Britt,[‡] Karel Base,[†]
Barbara Ramsay Shaw,[†] Anthony A. Ribeiro,[§] and Alvin L. Crumbliss[†]

Department of Chemistry, Duke University, Durham, North Carolina 27708, Department of Chemistry, University of California, Davis, California 95616, and Department of Radiology, Duke University Medical Center, Durham, North Carolina 27713

Received July 9, 2001

Methyl phosphite ((CH₃O)P(H)(O)₂⁻; MeOPH) and methylethyl phosphate ((CH₃O)P(OCH₂CH₃)(O)₂⁻; MEP) are two members of a class of anionic ligands whose ³¹P *T*₂ relaxation rates are remarkably sensitive to paramagnetic metal ions. The temperature dependence of the ³¹P NMR line broadenings caused by the Mn(H₂O)₆²⁺ ion and a water-soluble manganese(III) porphyrin (Mn^{III}TMPyP⁵⁺) indicates that the extent of paramagnetic relaxation enhancement is a measure of the rate at which the anionic probes come into physical contact with the paramagnetic center (i.e., enter the inner coordination shell); that is, $\pi\Delta\nu_{\text{par}} = k_{\text{assn}}[\text{M}]$, where $\Delta\nu_{\text{par}}$ is the difference between the line widths of the resonance in paramagnetic and diamagnetic solutions, and k_{assn} is the second-order rate constant for association of the phosphorus ligand with the metal, M. Comparison of the ³¹P *T*₁ and *T*₂ relaxation enhancements shows that rapid *T*₂ relaxation by the metal ion is caused by scalar interaction with the electronic spin. Relaxation of the phosphorus-bound proton of MeOPH (¹H–P) by Mn^{III}TMPyP⁵⁺ displayed intermediate exchange kinetics over much of the observable temperature range. The field strength dependence of ¹H–P *T*₂ enhancement and the independence of the ³¹P *T*₂ support these assertions. As in the case of the ³¹P *T*₂, the ¹H–P *T*₂ relaxation enhancement results from scalar interaction with the electronic spin. The scalar coupling interpretation of the NMR data is supported by a pulsed EPR study of the interactions of Mn(H₂O)₆²⁺ with the P-deuterated analogue of methyl phosphite, CH₃OP(²H)(O)₂⁻. The electron to ³¹P and ²H nuclear scalar coupling constants were found to be 4.6 and 0.10 MHz, respectively. In contrast, the effects of paramagnetic ions on the methoxy and ethoxy ¹H resonances of MeOPH and MEP are weak, and the evidence suggests that relaxation of these nuclei occurs by a dipolar mechanism. The wide variation in the relaxation sensitivities of the ¹H and ³¹P nuclei of MeOPH and MEP permits us to study how differences in the strengths of the interactions between an observed nucleus and a paramagnetic center affect NMR *T*₂ relaxations. We propose that these anion ligand probes may be used to study ligand-exchange reactivities of manganese complexes without requiring variable temperature studies. The ³¹P *T*₂ is determined by chemical association kinetics when the following condition is met: $(T_{2\text{M,P}}/T_{2\text{M,H}} - \Delta\nu_{\text{P}}/\Delta\nu_{\text{HP}} - 1) < 0.2$ where $T_{2\text{M,P}}$ and $T_{2\text{M,H}}$ are the transverse relaxation times of the ³¹P and ¹H nuclei when the probe is bound to the metal, and $\Delta\nu_{\text{P}}$ and $\Delta\nu_{\text{HP}}$ are the paramagnetic line broadenings of the ³¹P and ¹H–P nuclei, respectively. We assert that the ratio $T_{2\text{M,P}}/T_{2\text{M,H}}$ can be estimated for a general metal complex using the results of EPR and NMR experiments.

Introduction

Manganese ions play fundamental roles in metalloenzymes either by acting as divalent Lewis acids or by catalyzing redox reactions.^{1,2} In addition, many metalloenzymes that utilize other divalent metals (such as Mg²⁺, Ca²⁺, or Zn²⁺) retain significant

activity when Mn²⁺ is substituted for the native metal ion.^{3–5} Much of our understanding of the chemistry of metalloenzymes comes from studying the chemistry of relatively simple coordination complexes, including those of manganese.^{6,7}

* To whom correspondence should be addressed. Present address: Message Pharmaceuticals, Inc., 30 Spring Mill Drive, Malvern, PA 19355. E-mail: summers@messagepharm.com.

[†] Duke University.

[‡] University of California.

[§] Duke University Medical Center.

(1) Kessissoglou, D. P. In *Bioinorganic Chemistry*; Kessissoglou, D. P., Ed.; Kluwer Academic Publishers: The Netherlands, 1995; pp 299–320.

(2) Wieghardt, K. *Angew. Chem., Int. Ed. Engl.* **1989**, *28*, 1153–1172.

(3) Cohen, P. T. W.; Berndt, N. *Methods Enzymol.* **1991**, *201*, 408–427.

(4) Bertini, I.; Luchinat, C. In *Metal Ions in Biological Systems*; Sigel, H., Ed.; Marcel Dekker: New York, 1983; Vol. 15, pp 127–132.

(5) Sambrook, J.; Fritsch, E. F.; Maniatis, T. *Molecular Cloning, a Laboratory Manual*, 2nd ed.; Cold Spring Harbor Laboratory Press: Plainview, NY, 1989; p 5.35.

(6) Pecoraro, V. L. In *Manganese Redox Enzymes*; Pecoraro, V. L., Ed.; VCH Publishers: New York, 1992; pp 197–232.

(7) Pecoraro, V. L.; Gelasco, A.; Baldwin, M. J. In *Bioinorganic Chemistry*; Kessissoglou, D. P., Ed.; Kluwer Academic Publishers: The Netherlands, 1995; pp 287–298.

Manganese(II) complexes generally do not display pronounced electronic absorption spectra, making measurement of properties such as the ligand-exchange rates of manganese(II)-containing enzymes and model complexes difficult. Their high spins and relatively long spin-state lifetimes, however, confer many manganese complexes with strong magnetic relaxation enhancements.^{8,9} One of the aims of our laboratory is to exploit the dramatic effects that can be induced by paramagnetic metal ions on the NMR spectra of potential ligands^{10,11} to study the kinetics of metal/ligand exchange, as illustrated in eq 1



where PO represents the incoming ligand probe, and ML_N represents the metal complex.

Ligand-exchange reactions of many metal complexes occur by either dissociative or interchange mechanisms.¹² Dissociative-exchange kinetics (D) are, by definition, insensitive to the nucleophilicity of the incoming ligand. When this is the case, ligand-exchange rates gathered with one nucleophile should translate well to reactions with a broad range of nucleophiles. Interchange kinetics (I) can range from being nearly associative (I_a) to being nearly dissociative (I_d). The extent to which ligand nucleophilicity affects interchange kinetics is determined by the degree to which bond formation to the incoming ligand stabilizes the transition state.

The high relaxation enhancement of the Mn(II) ion has been exploited in paramagnetic proton relaxation enhancement (PRE) studies of proteins¹³ and nucleic acids.¹⁴ In PRE experiments, the relaxation enhancement of the solvent water ^1H resonance is used as an empirical measure to monitor changes in the metal ion chemical environment.^{9,15} The HOD resonance, however, is far from an ideal probe, in part because of its relatively low sensitivity to metal ions. The ^{17}O resonance of enriched water is more sensitive to metal ions but has seen limited use because of difficulties associated with quadrupolar ($\text{spin } 5/2$) nuclei and its low (0.04%) natural abundance. While the ^{19}F resonance of the fluoride ion is notable for its rapid relaxation by superoxide dismutase,¹⁶ this ion inactivates many metalloenzymes, presumably by competitive binding at the active site.

Correlating NMR line widths of ligand probes with their chemical-exchange kinetics will require probes with suitable

chemical and magnetic properties. For wide application in the study of metal ion-exchange kinetics, a probe must possess the following characteristics: (1) It must have at least one spin $1/2$ nucleus with a high receptivity¹⁷ and natural abundance. (2) This nucleus must interact strongly with the unpaired electron(s) when bound to the metal ion. (3) The lifetime of the metal/probe complex (τ_M) cannot be so long that the metal/probe complex is the major metal-containing species in solution. For the case of strong ligand binding, line broadening is determined by the rate of loss of the probe from the metal (eq 2, where PO^* is the displaced ligand) and is not a property of the native (nonbound) metal species, $(\text{H}_2\text{O})\text{ML}_N$. Additionally, strongly



binding ligands can induce changes in the nature of the metal ion, such as a high-spin to low-spin transition¹⁸ and the inhibition of enzymes.¹⁹

Early results in our laboratories indicate that certain phosphorus ester anions have properties that make them suitable candidates for probing the reactivities of paramagnetic metal complexes. The ^{31}P line widths of a number of phosphorus ester anions are determined by the rate at which the ion comes into physical contact with a variety of metal complexes, despite their relatively low thermodynamic binding affinity.²⁰ The fact that these probes have multiple observable nuclei provides an additional advantage that is discussed below. Using these probes, we plan to develop a method for determining ligand-exchange kinetics at paramagnetic metal ion sites such as those found in homogeneous catalysts and biologically important species. We call the method *Phosphorus Relaxation Enhancement* (PhoRE). In this report, we introduce two new probe ions, methyl phosphite ($(\text{CH}_3\text{O})\text{P}(\text{H})(\text{O})_2^-$; MeOPH) and methylethyl phosphate ($(\text{CH}_3\text{O})\text{P}(\text{OCH}_2\text{CH}_3)(\text{O})_2^-$; MEP), and we describe their interactions with two simple paramagnetic metal complexes, $\text{Mn}(\text{H}_2\text{O})_6^{2+}$ and a water-soluble manganese(III) porphyrin ($\text{Mn}^{\text{III}}\text{TMPyP}^{5+}$) (Figure 1).

Nuclei of ligands exchanging between paramagnetic (bound) and diamagnetic (free) environments frequently do not display a separate resonance for the bound ligand.²¹ Swift and Connick found that the observed line width is governed by the relative values of the mean lifetime of the metal/ligand complex (τ_M), the transverse relaxation time of the probe nucleus when bound to the paramagnetic metal ion (T_{2M}), the mean time the probe spends in solution before contacting the paramagnetic metal ion (τ_{sol}), and the difference between the precession frequencies of the ligand nuclei in the bound and free environments ($\Delta\omega_M$).²² Depending on how T_{2M} and $\Delta\omega_M$ compare to the rate of metal/

(8) Transverse and longitudinal relaxation enhancements (R_{2P} and R_{1P}) are the sensitivities of the magnetic T_2 or T_1 relaxation rate to metal ion concentration; R_{2P} is equal to the slope of a plot of $1/T_2$ versus metal ion concentration.

(9) (a) Koenig, S. H.; Brown, R. D.; Spiller, M. *Magn. Reson. Med.* **1987**, *4*, 252–260. (b) Abernathy, S. M.; Miller, J. C.; Lohr, L. L.; Sharp, R. R. *J. Chem. Phys.* **1998**, *109*, 4035–4046. (c) Kellar, K. E.; Foster, N. *Inorg. Chem.* **1992**, *31*, 1353–1359.

(10) Bertini, I.; Luchinat, C. *Coord. Chem. Rev.* **1996**, *150*, 1–296.

(11) Dwek, R. A. *Nuclear Magnetic Resonance in Biochemistry*; Clarendon Press: Oxford, 1973.

(12) Lincoln, S. F.; Merbach, A. E. *Adv. Inorg. Chem.* **1995**, *42*, 1–88.

(13) (a) Birkett, D. J.; Dwek, R. A.; Radda, G. K.; Salmon, A. G. *Eur. J. Biochem.* **1971**, *20*, 494–508. (b) Navon, G. *Chem. Phys. Lett.* **1970**, *7*, 390. (c) Mildvan, A. S.; Rosevear, P. R.; Granot, J.; O'Brian, C. A.; Bramson, H. N.; Kaiser, E. T. *Methods Enzymol.* **1983**, *99*, 93–119. (d) Mildvan, A. S.; Cohn, M. *Adv. Enzymol.* **1970**, *33*, 1–35.

(14) (a) Danchin, A.; Gueron, M. *J. Chem. Phys.* **1970**, *53*, 9, 3599–3609. (b) Peacocke, A. R.; Richards, R. E.; Sheard, B. *Mol. Phys.* **1969**, *16*, 177–189.

(15) Mildvan, A. S.; Engle, J. L. *Methods Enzymol.* **1972**, *26*, 654–683.

(16) (a) Rigo, A.; Ugo, P.; Viglino, P.; Rotilio, G. *FEBS Lett.* **1984**, *132*, 78–80. (b) Bracco, F.; Rigo, A.; Scarpa, M.; Viglino, P.; Battistin, L. In *PET and NMR, New Perspective in Neuroimaging and in Clinical Neurochemistry*; Battistin, L., Gerstenbrand, F., Eds.; Alan R. Liss, Inc.: New York, 1985; pp 315–324. (c) Rigo, A.; Viglino, P.; Argese, E.; Terenzi, M.; Rotilio, G. *J. Biol. Chem.* **1979**, 1759–1760. (d) Viglino, P.; Rigo, A.; Stevanto, R.; Ranieri, G. A. *J. Magn. Reson.* **1979**, *34*, 265–274.

(17) Yoder, C. H.; Schaeffer, C. D. *Introduction to Multinuclear NMR*; The Benjamin/Cummings Publishing Co., Inc.: Menlo Park, CA, 1987; p 28.

(18) (a) Morishima, I.; Inubushi, T. *J. Am. Chem. Soc.* **1978**, *100*, 3568–3578. (b) Shiro, Y.; Iizuka, T.; Makino, R.; Ishimura, Y.; Morishima, I. *J. Am. Chem. Soc.* **1989**, *111*, 7707–7711. (c) Banci, L.; Bertini, I.; Kuan, I. C.; Tien, M.; Turano, P.; Vila, A. J. *Biochemistry* **1993**, *32*, 13483–13489.

(19) (a) Khangulov, S. V.; Barynin, N. N.; Antonyuk-Barynina, S. V. *Biochim. Biophys. Acta* **1990**, *1020*, 25–33. (b) Haddy, A.; Hatchellk, J. A.; Kimel, R. A.; Thomas, R. *Biochemistry* **1999**, *38*, 6104–6110. (c) Baumgarten, M.; Philo, J. S.; Dismukes, G. C. *Biochemistry* **1990**, *29*, 10814–10822.

(20) Summers, J. S.; Base, K.; Boukhalfa, H.; Shaw, B. R.; Crumbliss, A. L. Unpublished work.

(21) (a) McConnell, H. M. *J. Chem. Phys.* **1958**, *28*, 430–431. (b) Bernheim, R. A.; Brown, T. H.; Gutowsky, H. S.; Woessner, D. E. *J. Chem. Phys.* **1959**, *30*, 950–956. (c) Rubenstein, M.; Baram, A.; Luz, Z. *Mol. Phys.* **1971**, *20*, 67.

(22) Swift, T. J.; Connick, R. E. *J. Chem. Phys.* **1962**, *37*, 307–320.

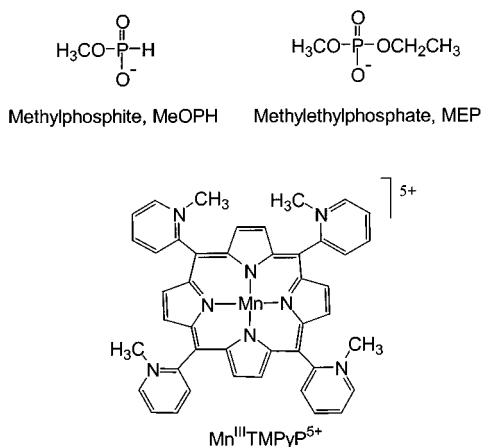


Figure 1. Structures of MEP, MeOPH, and Mn^{III}TMPyP⁵⁺.

probe complex dissociation ($1/\tau_M$), line widths can be approximated by one of two limiting behaviors or may be intermediate between the two. For manganese complexes, where values of $1/T_{2M}$ are generally much greater than $\Delta\omega_M$, the Swift and Connick equation for the paramagnetic contribution to the transverse relaxation time ($T_{2,par}$) reduces to eq 3²³

$$\pi\Delta\nu_{par} = 1/T_{2,par} = (1/\tau_{sol})(1/T_{2M})/(1/\tau_M + 1/T_{2M}) \quad (3)$$

where $\Delta\nu_{par}$ is the difference in the line widths of the probe resonance in paramagnetic and diamagnetic solutions. If the transverse relaxation rate is much greater than the rate at which the metal/ligand complex dissociates ($1/T_{2M} \gg 1/\tau_M$), the system is in what is frequently referred to as slow exchange, and eq 3 reduces to eq 4

$$\pi\Delta\nu_{par} = (1/\tau_{sol}) = (k_{assn})[M] \quad (4)$$

where $[M]$ is the concentration of the metal complex, and k_{assn} is the rate constant for the ligand association reaction, eq 1. When this condition holds, metal/ligand association kinetics are easily determined from line width data. If $1/\tau_M \gg 1/T_{2M}$, however, the observed line widths are determined by eq 5. The

$$\pi\Delta\nu_{par} = (\tau_M/\tau_{sol})1/T_{2M} \quad (5)$$

existence of two limiting and one intermediate behaviors means that no rate or equilibrium data can be extracted from a change in a ligand line width without additional information.^{10,11,21}

Ligand-exchange rates for a wide variety of ligands were determined by NMR. Typically, relaxation rates and line shifts are measured over as wide a temperature range as possible, and the data are treated to extract the kinetic parameters.^{24,25} Many systems of interest (such as metal complexes of biopolymers), however, are not amenable to study at the extremes of temperature needed to establish whether slow-exchange conditions hold. To establish criteria for correlating the ³¹P transverse relaxation enhancements (defined as the molar effect of a metal complex on the paramagnetic relaxation rate; $R_{2p} = \delta(1/T_{2,par})/\delta[M]$) with metal ion/ligand association rate constants, we have studied how paramagnetic ions affect the T_1 and T_2 values of

different nuclei of two of our probe ion candidates, MeOPH and MEP. The ¹H and ³¹P nuclei of these ions behave very differently from each other, making it possible to study how differences in the properties of the observed nuclei affect line widths under identical conditions of exchange rate, temperature, and pH. These studies allow us to determine when MeOPH and MEP may be used as probes of the reactivities of paramagnetic metal ions toward inner shell coordination exchange without requiring variable temperature studies.

Experimental Section

Preparation of Samples. Samples of MeOPH ((CH₃O)P(H)(O)₂⁻) were prepared as the sodium salt by partial hydrolysis of dimethyl phosphite, (CH₃O)₂P(H)O, in aqueous NaOH. Methylene phosphate (MEP) was prepared by reaction of dichloroethyl phosphate, (CH₃-CH₂O)P(O)(Cl)₂, with 10:1 v/v methanol/water mixture. The anionic monomethyl ester product was separated from the neutral diester by extraction from CHCl₃ solution with aqueous diisopropylamine solution. The MEP anion was isolated as the diisopropylammonium salt. The chloride salt of 5,10,15,20-tetrakis(*N*-methylpyridinium-2-yl)porphyrin manganese(III) (Mn^{III}TMPyP⁵⁺) (Irwin Fridovich, Duke University) and manganese(II) sulfate (Sigma) were used without further purification.

Samples for NMR spectroscopic T_1 and T_2 analysis were prepared by mixing an aliquot of a stock D₂O solution (containing the sodium salt of the phosphorus probe, tetramethylphosphonium chloride reference, and acetate buffer) with aliquots of metal complex solution (either MnSO₄ or Mn^{III}TMPyP⁵⁺ in D₂O) and sufficient D₂O to bring the final volume to 600 μ L. Stock solutions were prepared as follows: Weighed samples of the diisopropylammonium salt of MEP were converted to the sodium salt by treatment with a slight excess of NaOH solution, and the resulting solution was evaporated to dryness. The residues were taken into acetate-buffered D₂O containing a known concentration of the tetramethyl phosphonium (Me₄P⁺) reference, and the pH was adjusted to pH \approx 5 with 1 N deuterated acetic acid (prepared by reaction of acetic anhydride with D₂O). The solution pH values were determined from the chemical shift of the acetate hydrogen resonance relative to the proton resonance of Me₄P⁺. The final concentrations for experiments with the MeOPH probe were 17 mM MeOPH and 10 mM Me₄P⁺ reference in 4 mM acetate, pH 5.13. The MEP samples contained 8.3 mM MEP and 5.5 mM Me₄P⁺ in 3.4 mM acetate, pH 5.06. Final concentrations of acetate and probe were calculated from the integrated intensities of their proton resonances using the known concentration of the reference ion. Metal-containing solutions were prepared by serial dilution of stock solutions prepared from weighed samples. Final metal concentrations for determination of the effect of Mn(H₂O)₆²⁺ on the MeOPH T_2 values were 1.0, 2.0, and 3.0 μ M for the CPMG method²⁶ and 8.0 and 40 μ M for the line width method. For the Mn^{III}TMPyP⁵⁺/MeOPH system, metal concentrations were 0.75, 1.50, and 2.25 μ M (CPMG) and 12 and 36 μ M (line width method). MEP measurements used the CPMG method with solutions containing 3.5, 7.0, and 10.5 μ M Mn(H₂O)₆²⁺ and 5.0, 10.0, and 20 μ M Mn^{III}TMPyP⁵⁺. The concentration of Mn^{III}TMPyP⁵⁺ in the stock solution was determined spectrophotometrically, and the concentrations of samples prepared from it were calculated accordingly.

Enthalpies of activation for transverse relaxation were determined from the plots of line width versus metal concentration at temperatures ranging from 5 to 85° C. The diamagnetic ³¹P line width of MeOPH increases dramatically with temperature limiting the accuracy of measurements made at higher temperatures. Measurements were made on solutions for each metal complex. For the Mn^{III}TMPyP⁵⁺ experiments, metal complex concentrations were 0, 3.7, 9.3, and 32 μ M. For Mn(H₂O)₆²⁺, concentrations were 0, 2.2, 4.7, and 7.9 μ M. The slopes of the linear portions of plots of $\ln(R_{2p}/T)$ versus $1/T$ were used to determine enthalpies of activation.

Instrumentation. The majority of NMR spectra were recorded using a Varian Inova 400 MHz NMR spectrometer at a field strength of 9.40

- (23) A fuller treatment of the approximations made in this analysis is presented in the Supporting Information section of this paper which is available online.
 (24) Duccomon, Y.; Newman, K. E.; Merbach, A. E. *Inorg. Chem.* **1980**, *19*, 3696–3703.
 (25) Stengle, T. R.; Langford, C. H. *Coord. Chem. Rev.* **1967**, *2*, 349–370. Hunt, J. P. *Chem. Rev.* **1971**, *71*, 1–10. Lauffer, R. B. *Chem. Rev.* **1987**, *87*, 901.

- (26) Friebolin, H. *Basic One- and Two-Dimensional NMR Spectroscopy*, 2nd ed.; VCH Publishers: Weinheim, 1993.

T. The T_2 values of the MeOPH sample containing 3.8 μM Mn^{III} -TMPyP $^{5+}$ were also measured at 11.75 T using a Varian Unity Plus 500 MHz and at 7.05 T with a Varian Mercury 300 MHz NMR spectrometer.

NMR Procedures. ^{31}P and ^1H T_2 values for MeOPH and MEP were determined by the CPMG technique²⁶ and from line width data. For each probe ion, CPMG T_2 values were measured in the absence of added metal complex and at three concentrations each of $\text{Mn}(\text{H}_2\text{O})_6^{2+}$ and Mn^{III} -TMPyP $^{5+}$. T_2 values were calculated from the slopes of the linear plots of $\ln(I/I_0)$ versus time. R^2 values for the 400 MHz data averaged 0.993 and never fell below 0.980. T_1 values were determined for a representative sample of each probe with each metal complex using the standard inversion recovery method. For MeOPH, the 3.0 μM $\text{Mn}(\text{H}_2\text{O})_6^{2+}$ and 2.25 μM Mn^{III} -TMPyP $^{5+}$ solutions were used to determine T_1 metal relaxation enhancements ($R_{1\text{P}}$). For MEP T_1 measurements, metal concentrations were 10.5 μM $\text{Mn}(\text{H}_2\text{O})_6^{2+}$ and 20 μM Mn^{III} -TMPyP $^{5+}$.

At higher metal ion concentrations, the effects of the metal ion on line widths are much larger than the effects of field inhomogeneities, and T_2 values are more conveniently determined from line width data. Broadening of the ^{31}P resonance of the Me_4P^+ reference ion by the metals was negligible. The line width of this resonance was used to compensate for field inhomogeneities, eq 6

$$1/T_{2\text{par}} - 1/T_{2\text{dia}} = \pi[(\Delta\nu_{\text{par}})_{\text{probe}} - (\Delta\nu_{\text{par}})_{\text{ref}}] \quad (6)$$

where $\Delta\nu_{\text{par}}$ refers to the difference between the full width at half-heights of the resonance in the presence and absence of the paramagnetic ion, and the subscripts "probe" and "ref" refer to the resonances of the probe and reference ions, respectively.

Pulsed EPR Spectroscopy. Electron spin-echo envelope modulation (ESEEM) and electron spin-echo-electron nuclear double resonance (ESE-ENDOR) experiments were performed on a laboratory-built X-band pulsed ENDOR spectrometer.²⁷ All spectroscopy was performed in frozen solution at 4.2 K. Samples contained 1 mM Mn(II), 1 M phosphite ligand as specified, 20 mM acetate buffer, pH 5.0, and 0.4 M sucrose as a cryoprotectant. The static field was set to a maximum of the six-line Mn(II) EPR spectrum. Three-pulse ESEEM spectra^{28,29} were obtained on samples of Mn(II) in $(\text{CH}_3\text{O})\text{P}(\text{H})(\text{O})_2^- \text{K}^+$ or $(\text{CH}_3\text{O})\text{P}(\text{D})(\text{O})_2^- \text{K}^+$ at a microwave frequency of 9.3 GHz. The deuteration level of the $(\text{CH}_3\text{O})\text{P}(\text{H})(\text{O})_2^-$ sample was determined using NMR, and the number of phosphite ligands to each Mn(II) was determined by counting waters of hydration via comparison of ESEEM spectra for the protonated species in D_2O and H_2O and by assuming octahedral Mn(II).³⁰ These values were taken into account in the interpretation of ESEEM data (see below). For ^{31}P , ESE-ENDOR spectra were obtained on protonated samples using the method of Mims³¹ at a microwave frequency of 10.2 GHz using an rf pulse length of 8 μs and spin-echo delays (τ) of 180, 275, and 450 ns. For ^2H , Mims ESE-ENDOR spectra were obtained at 10.2 GHz using a τ of 800 ns and an rf pulse length of 16 μs .

Experimental data were baseline-corrected using linear or quadratic functions and inverted in phase for display. Simulations reflect the τ -dependent suppression effect, which convolves the ENDOR line shape with a sinusoidal function centered at the nuclear frequency with period τ^{-1} .³² Final simulations were performed with the hyperfine parameters in Table 3, an e^2qQ value of 0.21 and $\eta = 0.0$ for ^2H and Gaussian line shape functions with $a = 30$ kHz for ^{31}P and 8 kHz for ^2H .

(27) (a) Sturgeon, B. E.; Britt, R. D. *Rev. Sci. Instrum.* **1988**, *63*, 2187–2192. (b) Sturgeon, B. E.; Ball, J. A.; Randall, D. W.; Britt, R. D. *J. Phys. Chem.* **1994**, *98*, 12871–12883.

(28) Mims, W. B.; Peisach, J. In *Biological Magnetic Resonance*; Berliner, L. J., Ruben, J., Eds.; Plenum Press: New York, 1981; Vol. 3, pp 213–263.

(29) Britt, R. D. *Curr. Opin. Struct. Biol.* **1993**, *3*, 774–779.

(30) Serpersu, E. H.; McCracken, J.; Peisach, J.; Mildvan, A. S. *Biochemistry* **1988**, *27*, 8034–8044.

(31) Mims, W. B. *Proc. R. Soc. London, Ser. A* **1965**, *283*, 452–457.

(32) Hoffman, B. M.; DeRose, V. J.; Doan, P. E.; Gurbel, R. J.; Houseman, A. L. P.; Telser, J. In *Biological Magnetic Resonance*; Berliner, L. J., Ruben, J., Eds.; Plenum Press: New York, 1993; Vol. 13, pp 151–217.

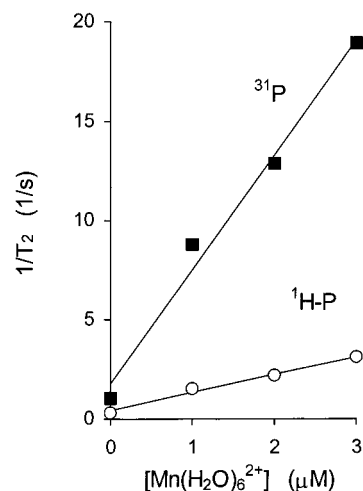


Figure 2. The effects of $[\text{Mn}(\text{H}_2\text{O})_6^{2+}]$ on the T_2 relaxation rate of the ^1H -P (open circles) and ^{31}P (filled squares) resonances of $(\text{CH}_3\text{O})\text{P}(\text{H})(\text{O})_2^-$ as determined by the CPMG technique. Solutions contained 17 mM MeOPH, 10 mM Me_4P^+ , and 4 mM acetate, pH 5.13, 25 °C.

The dipolar component of the electron–nuclear hyperfine tensor (A_{dip}) for ^2H was determined by measuring the depth of modulation in a ratio of three-pulse ESEEM data taken on deuterated vs protonated methyl phosphite.³³ An r^{-6} dependence of modulation depth on A_{dip} was assumed,³⁴ and the data were calibrated using a complex of $\text{Mn}^{\text{II}}\text{EDTA}^-$ compared to $\text{Mn}^{\text{II}}\text{DTPA}^{2-}$ in D_2O vs H_2O as a standard for modulation due to two deuterons at a point–dipole distance of 2.9 Å. Error limits were determined by repeating the analysis at three magnetic fields within the Mn(II) EPR spectral envelope. Scalar (A_{iso}) and dipolar components of the electron–nuclear hyperfine tensor for ^{31}P , as well as A_{iso} for ^2H , were determined by simulation of ESE-ENDOR spectra assuming an axially symmetric hyperfine tensor and neglecting the outer manifolds of the $S = 5/2$ Mn(II) ion.^{28,35} Error limits represent the spread of parameters giving acceptable fits of simulations to experimental data.

Results

Transverse relaxation rates ($1/T_2$) of each of the ^{31}P and ^1H resonances of MeOPH and MEP (determined by both the CPMG^{17,26} technique and from line widths) increased linearly with $\text{Mn}(\text{H}_2\text{O})_6^{2+}$ and Mn^{III} -TMPyP $^{5+}$ complex concentration. The results from CPMG experiments on the effect of $\text{Mn}(\text{H}_2\text{O})_6^{2+}$ on the T_2 values of the ^{31}P and ^1H -P resonances of MeOPH are typical and are shown in Figure 2. Values determined from line width data at higher metal concentrations were consistent with values determined by the CPMG technique.³⁶ The relaxation enhancements of the two metal complexes (calculated as the slopes of plots of $1/T_{2\text{par}}$ versus $[\text{M}]$ or as $(1/T_{1\text{par}})/[\text{M}]$) toward the ^1H and ^{31}P resonances of MeOPH are presented in Table 1. The same data for the resonances of MEP are presented in Table 2. The effects on the resonances of the reference were too small to measure under our experimental conditions.

The ^{31}P relaxation enhancements of both of the probe ions by both of the metal complexes increased linearly with

(33) Mims, W. B.; Davis, J. L.; Peisach, J. *J. Magn. Reson.* **1990**, *86*, 273–292.

(34) Kevan, L. In *Time Domain Electron Spin Resonance*; Kevan, L., Schwartz, R. N., Eds.; John Wiley & Sons: New York, 1979; pp 279–341.

(35) Randall, D. W.; Gelasco, A.; Caudle, M. T.; Pecoraro, V. L.; Britt, R. D. *J. Am. Chem. Soc.* **1997**, *119*, 4481–4491.

(36) Individual data are not presented. Relaxation times for individual experiments are tabulated in the supplementary information section of this paper, which can be accessed online.

Table 1. Molar Relaxation Enhancements^a of Mn(H₂O)₆²⁺ and Mn^{III}TMPyP⁵⁺ toward the ³¹P and ¹H–P Resonances of MeOPH (CH₃OP(H)O₂⁻) and Activation Enthalpies for Metal Probe Association^b

complex	³¹ P R _{2p} × 10 ⁻⁶ (M ⁻¹ s ⁻¹)	ΔH [‡] (kcal/mol)	³¹ P R _{1p} × 10 ⁻⁶ (M ⁻¹ s ⁻¹)	¹ H–P R _{2p} × 10 ⁻⁶ (M ⁻¹ s ⁻¹)	¹ H–P R _{1p} × 10 ⁻⁶ (M ⁻¹ s ⁻¹)
Mn(H ₂ O) ₆ ²⁺	5.8	11.3	0.038	0.73	0.064
Mn ^{III} TMPyP ⁵⁺	2.1	8.7	0.56	1.14	0.16

^a Transverse and longitudinal relaxation enhancements (R_{1p} and R_{2p}) are the slopes of plots of 1/T₂ or 1/T₁ versus metal concentration, respectively.
^b Activation enthalpies calculated from the slopes of the linear regions of plots of ln(³¹P R_{2p}/T) versus 1/T.

Table 2. Molar Relaxation Enhancements of Mn(H₂O)₆²⁺ and Mn^{III}TMPyP⁵⁺ toward the ³¹P (R_{2p} and R_{1p} × 10⁻⁶ M⁻¹ s⁻¹) and ¹H (R_{2p}) Resonances of MEP (CH₃OP(OCH₂CH₃)O₂⁻) and Activation Enthalpies for Relaxation

	³¹ P R _{2p} × 10 ⁻⁶ (M ⁻¹ s ⁻¹)	ΔH [‡] (kcal/mol)	³¹ P R _{1p} × 10 ⁻⁶ (M ⁻¹ s ⁻¹)	OC ¹ H ₂ CH ₃ R _{2p} × 10 ⁻⁶ (M ⁻¹ s ⁻¹)	OCH ₂ C ¹ H ₃ R _{2p} × 10 ⁻⁶ (M ⁻¹ s ⁻¹)	OC ¹ H ₃ R _{2p} × 10 ⁻⁶ (M ⁻¹ s ⁻¹)
Mn(H ₂ O) ₆ ²⁺	3.9	8.2	0.11	0.029	0.013	0.014
Mn ^{III} TMPyP ⁵⁺	1.2	8.2	0.62	0.063	0.040	0.048

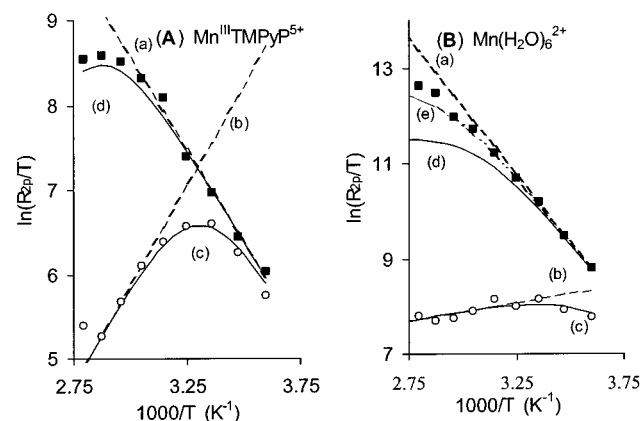


Figure 3. The effects of temperature on the paramagnetic line broadening of the ¹H–P (open circles) and ³¹P (filled squares) resonances of (CH₃O)P(H)(O)₂⁻ by Mn^{III}TMPyP⁵⁺ (A) and Mn(H₂O)₆²⁺ (B). Dashed lines represent the behavior predicted (a) for πΔν_{par} = 1/τ_{sol} or (b) for πΔν_{par} = (τ_M/τ_{sol})/T_{2MH}. Line c represents the ¹H–P Δν predicted from the limiting behaviors. Line d represents the ³¹P Δν predicted by assuming T_{2MP} is related to T_{2MH} by the coupling constants in Table 3. Line e in (B) represents the behavior predicted at the upper limit of the reported uncertainty in the EPR data: A_p = (A_{iso} + σA_{iso}), A_H = (A_{iso} - σA_{iso}).}

temperature over most of the accessible range. A plot of ln(R_{2p}/T) versus 1/T for the phosphite ¹H–P and ³¹P resonances broadened by Mn^{III}TMPyP⁵⁺ as a function of temperature is presented in Figure 3A. The plot for the relaxation of the MeOPH resonances by Mn(H₂O)₆²⁺ is presented as Figure 3B. At high temperatures, the ³¹P line widths deviated significantly from those predicted by the kinetic model. This behavior is consistent with the expected switch to an intermediate kinetic regime, where the ligand-exchange rate is no longer the sole factor determining metal relaxation enhancement. Slopes from the linear portions of ln(R_{2p}/T) versus 1/T plots gave the activation enthalpies presented in Tables 1 and 2.

Paramagnetic broadening of the ¹H–P resonance approached that of the ³¹P resonance only for Mn^{III}TMPyP⁵⁺ and only at low temperature. As seen in Figure 3A, the ¹H–P line width increases with temperature to a maximum value, after which the line width decreased with increasing temperature. At all temperatures, Mn(H₂O)₆²⁺ broadened the MeOPH ³¹P resonance much more than the ¹H–P resonance, Figure 3B. While ³¹P T₂ relaxation enhancements were insensitive to changes in instrument field strength, the ¹H–P T₂ relaxation enhancements of the two metal ions decreased with increasing field. The field strength dependence of the MeOPH ¹H–P and ³¹P relaxation enhancements by Mn^{III}TMPyP⁵⁺ is presented in Figure 4. The effects of temperature and field strength on line broadening of

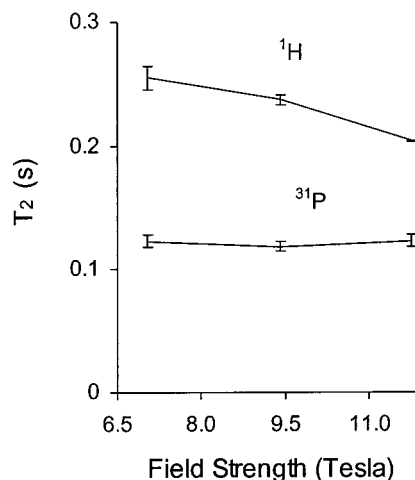


Figure 4. Dependence of the T₂ relaxation enhancements of the ¹H–P (upper data) and ³¹P (lower data) resonances of MeOPH on instrument field strength.

the alkyl resonances were not monitored since changes in the widths of these lines were small.

Metal electron to ligand nuclear hyperfine coupling constants were investigated using ENDOR and ESEEM spectroscopies. A series of simulated spectra were prepared using different values of A_{iso} and A_{dip} and were compared to the measured spectra. The values that gave the best fit to the data are presented in Table 3. A portion of the measured spectra are presented in Figure 5, along with simulated spectra predicted using the values in Table 3. The observed and simulated spectra are in good agreement. Distances calculated from dipolar hyperfine contributions (using the point–dipole approximation) are chemically reasonable.³⁷

Discussion

The ¹H–P and ³¹P line broadening data for both manganese complexes are well described by eq 3, assuming that t_{sol}, t_M, and T_{2M} obey Arrhenius behavior. The dashed line a in Figure 3A and B represents the behavior predicted when the line widths are limited by exchange kinetics, described by eq 4. Line b shows the limiting behavior of the ¹H resonance under rapid exchange, described by eq 5. Solid line c shows the behavior predicted for the ¹H–P resonance by eq 3 using the parameters that define lines a and b. Note that the ¹H and ³¹P measurements were recorded on the same samples under identical chemical conditions. With the exception of T_{2M}, the variables that define

(37) Comparison to methyl phosphite zinc adduct: Weis, K.; Rombach, M.; Ruf, M.; Vahrenkamp, H. *Eur. J. Inorg. Chem.* **1998**, 263–270.

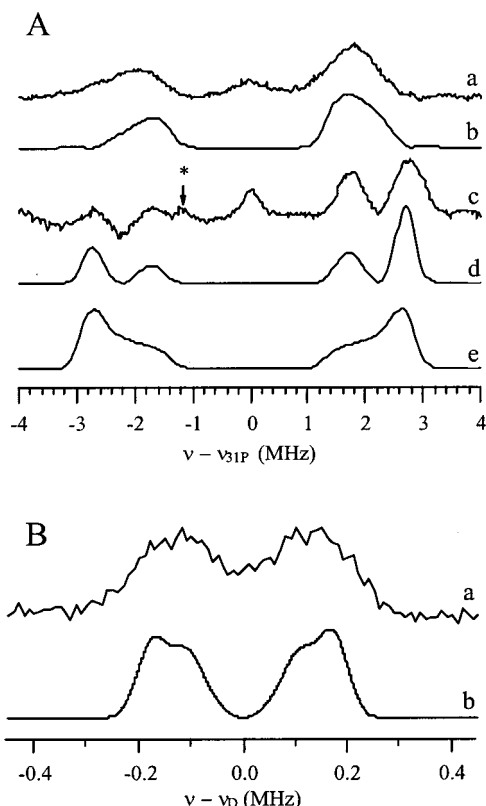


Figure 5. Hyperfine coupling constant analysis of the manganese(II)/MeOPH complex using ESE-ENDOR. Samples contained 1 mM Mn(II), 1 M MeOPH, 20 mM acetate buffer, pH 5.0, and 0.4 M sucrose. Experimental ^{31}P ESE-ENDOR spectra at τ delays of 180 ns and 450 ns (A, traces a, c) are simulated in traces b and d. Trace e is the reconstructed ENDOR line shape that would be observed in the absence of τ -dependent effects. The asterisk indicates an overtone at $1/3$ the frequency of the intense ^1H (solvent) line. Experimental and simulated ^2H ESE-ENDOR spectra are presented in (B), traces a and b, respectively. For both nuclei, unsimulated intensity at $\nu - \nu_n = 0$ arises from nonspecific or "distant" ENDOR interactions with nuclei elsewhere in the sample.²⁸

Table 3. Hyperfine Coupling Data for $((\text{CH}_3\text{O})^{31}\text{P}(\text{O})\text{O})\text{Mn}(\text{OH}_2)_5^+$

nucleus	hyperfine coupling constants (MHz)		distance ^a (Å)
	A_{iso} (scalar)	A_{dip} (dipolar)	
^{31}P	4.6 ± 0.3	1.0 ± 0.2	3.2 ± 0.2
^2H	0.10 ± 0.04	0.18 ± 0.02	4.1 ± 0.2

^a Distances calculated from dipolar coupling constants assuming r^{-6} dependence.

the width of the ^1H resonance also define that of the ^{31}P resonance. Line d in Figure 3A and B shows the behavior predicted for the ^{31}P resonance using the above parameters and assuming $T_{2\text{M}}$ of the ^{31}P is related to $T_{2\text{M}}$ of the ^1H -P by the isotropic coupling constants (A_{iso}) obtained in our EPR studies, Table 3. The upward displacement of the ^{31}P data from line d at the high-temperature end of Figure 3B suggests that the ratio of ^1H -P to ^{31}P A_{iso} under the conditions of the NMR experiments is lower than that measured by EPR. We note that the EPR and NMR measurements are made under extremely different conditions of concentration and temperature. As such, the difference in the predicted and observed behaviors may be due to differences in the speciation of the metal ion under the two sets of experimental conditions. Surprisingly, the Mn^{III} -TMPyP $^{5+}$ data fit that which was predicted by the Mn^{2+} A_{iso} values better than that of the $\text{Mn}(\text{H}_2\text{O})_6^{2+}$.

For most of the accessible temperature range (below ~ 65 °C), the ^{31}P line broadenings of MeOPH and MEP are approximately those predicted by eq 4, line a in Figure 3A and B. Under this condition, line widths equal the rate at which the metal and probe ions come into contact. From these observations, we conclude that the ^{31}P $R_{2\text{P}}$ (25 °C) values reported in Tables 1 and 2 are equal to the second-order rate constants for ligand exchange in these systems. We believe that water substitution is the dominant reaction (eq 1) and not exchange of the bound probe ion (eq 2). Equilibrium measurements show that metal/probe complexes account for only a small percentage of total metal under the conditions we employed.³⁸ A ligand-exchange rate constant (k_{calc}) may be calculated for $\text{Mn}(\text{H}_2\text{O})_6^{2+}$ using eq 7³⁹

$$k_{\text{calc}} = SK_{\text{os}}k_{\text{H}_2\text{O}} \quad (7)$$

where S is a statistical factor ($1/6$), $k_{\text{H}_2\text{O}}$ is the water-exchange rate, and K_{os} is the outer sphere complex formation constant. Using the literature value for $k_{\text{H}_2\text{O}}$ ($2.1 \times 10^7 \text{ s}^{-1}$)³⁹ and a value of K_{os} predicted by a simple electrostatic model (2 M^{-1}) gives a value of k_{calc} ($7 \times 10^6 \text{ M}^{-1} \text{ s}^{-1}$) that compares well to our measured values for k_{assn} (5.8×10^6 and $3.9 \times 10^6 \text{ M}^{-1} \text{ s}^{-1}$ for reaction of $\text{Mn}(\text{H}_2\text{O})_6^{2+}$ with MeOPH and MEP, respectively, Tables 1 and 2). The measured k_{assn} values for the reaction of Mn^{III} -TMPyP $^{5+}$ with MeOPH and MEP are 2.1×10^6 and $1.2 \times 10^6 \text{ M}^{-1} \text{ s}^{-1}$, respectively (Tables 1 and 2). While significantly smaller rate constants are expected for ligand exchange at a Mn^{3+} ion relative to a Mn^{2+} ion,⁴⁰ our observed rate constants were similar for $\text{Mn}(\text{H}_2\text{O})_6^{2+}$ and Mn^{III} -TMPyP $^{5+}$. Reactions of Mn^{III} -TMPyP $^{5+}$ are undoubtedly accelerated by the porphyrin ligand environment and the overall 5+ charge on the complex.

Comparison of ^{31}P T_1 and T_2 Relaxation Enhancements ($R_{1\text{P}}$ and $R_{2\text{P}}$). We found that ^{31}P T_1 relaxation was much less sensitive to the metal ions than ^{31}P T_2 relaxation (Tables 1 and 2). For $\text{Mn}(\text{H}_2\text{O})_6^{2+}$, the MeOPH ^{31}P $R_{1\text{P}}$ and $R_{2\text{P}}$ differed by more than 2 orders of magnitude. Complex dissociation is, therefore, slow compared to T_2 relaxation but is rapid compared to T_1 relaxation. While Swift and Connick predict slow exchange when either $1/T_{2\text{M}}$ or $\Delta\omega_{\text{M}}$ is much greater than $1/\tau_{\text{M}}$, earlier researchers concluded that $1/T_{2\text{M}} > \Delta\omega_{\text{M}}$ for manganese(II) complexes if reasonable coupling constant and τ_{e} values are assumed.^{22,24} The difference in the measured ^{31}P (and also ^1H) T_2 and T_1 relaxation rates, therefore, indicates substantial differences in $T_{1\text{M}}$ and $T_{2\text{M}}$. For small molecular ions with short rotational correlation times, the Solomon-Bloembergen equations^{10,11} only predict this behavior when scalar coupling contributes significantly to $T_{2\text{M}}$.²³

$$1/T_{2\text{M},\text{scalar}} - (1/2)1/T_{1\text{M},\text{scalar}} = (1/3)S(S+1)(2\pi A)^2\{\tau_{\text{e}}\} \quad (8)$$

While we are not aware of other published coupling constants for metal/phosphite complexes, our values are in good agreement with coupling constants reported for metal phosphate com-

(38) Equilibrium binding constants were found to be less than 3 M^{-1} for any combination of metal complex and probe ions employed. These data will be published elsewhere.

(39) (a) Wilkins, R. G. *Study of Kinetics and Mechanism of Reactions of Transition Metal Complexes*; VCH Publishers: New York, 1991. (b) Lincoln, S. F.; Merback, A. E. *Adv. Inorg. Chem.* **1995**, *42*, 1–88. (c) Frey, C. M.; Stuehr, J. In *Metal Ions in Biological Systems*; Sigel, H., Ed.; Marcel Dekker: New York, 1974; Vol. 1, pp 52–116.

(40) Pecoraro, V. L. In *Manganese Redox Enzymes*; VCH Publishers: New York, 1992; pp 1–28.

plexes.⁴¹ The 4.6 MHz value we report is consistent with slow exchange mediated via a T_{2M} relaxation if reasonable values are presumed for the lifetimes of the electronic spin (10^{-8} s)¹⁰ and the metal/probe complex.

The change from the slow- to the rapid-exchange regime on switching from monitoring the ³¹P T_2 to the T_1 is accompanied by a reversal in the order of the metal ion relaxation enhancements; while the ³¹P T_2 was more sensitive to $Mn(H_2O)_6^{2+}$, the ³¹P T_1 was more sensitive to $Mn^{III}TMPyP^{5+}$. We note that slow-exchange relaxation is governed by chemical kinetics ($1/T_{2par} \propto k_{assn}$), while relaxation in rapid exchange is governed by chemical thermodynamics ($1/T_{1par} \propto K_{eq}$). While it is tempting to attribute the difference in T_1 relaxation enhancements to differences in binding constants, differences in electron spin relaxation rates of the two complexes may also contribute to the effect.

Relaxation of the ¹H–P Nucleus. Three lines of reasoning suggest that fundamentally different factors influence T_2 relaxations of the phosphite ¹H–P and ³¹P nuclei at room temperature. First, the temperature dependence of the phosphite ¹H–P line width is markedly different than that of the ³¹P resonance, Figure 3. Second, the ¹H–P T_2 relaxation enhancement decreased with increasing field strength while the ³¹P relaxation enhancement did not, Figure 4. Third, the R_{2p} of the ¹H–P resonance was greater for $Mn^{III}TMPyP^{5+}$ than for $Mn(H_2O)_6^{2+}$, while the opposite was true for the ³¹P resonances (this ordering was also observed for the ³¹P R_{1p} and for the R_{1p} and R_{2p} values of all other ¹H resonances).

The temperature dependence of the ¹H–P line broadening by $Mn^{III}TMPyP^{5+}$ indicates that this resonance undergoes intermediate T_2 relaxation kinetics (i.e., $T_{2M} \approx \tau_M$) over much of the observed temperature range. At low temperatures (where τ_M is the longest), the ¹H–P line width approached that of the ³¹P resonance, indicating slow-exchange behavior. At the highest temperatures, the line width behavior decreases with increasing temperature, as expected for a ligand undergoing fast exchange. Between these extreme regions, phosphite coordination to the $Mn^{III}TMPyP^{5+}$ occurs with intermediate kinetics.

Like the ³¹P resonance, the ¹H–P R_{1p} and R_{2p} values differed by more than a factor of 10 for each metal complex (Table 1), indicating strong scalar coupling of the electron spin to this nucleus (see above). This conclusion was supported by the 0.10 MHz scalar contribution to the electron/deuterium hyperfine coupling we found by ESEEM. The field strength dependence of the ¹H–P T_{2par} , therefore, results from the field strength dependence of τ_c .⁴² The weaker coupling of the ²H–P nucleus explains how the ³¹P resonance can be in slow exchange under conditions where the ¹H–P resonance is in intermediate exchange.

Effects of Metal Ions on MEP Alkoxy ¹H Resonances.

We examined the relaxation enhancements of the ¹H resonances of MEP to study the importance of scalar coupling to groups at the periphery of the probe ion. While metal ions had little influence on the methoxy (¹H₃CO) hydrogen resonance of MeOPH, the origin of the difference between the effects on the ¹H–P and ¹H₃CO resonance was unclear. We expected scalar coupling between the ¹H nuclei and the unpaired electrons in

the metal complex to be influenced by the same factors that affect the J_{PH} coupling constants. Since the coupling constants for the ¹H–P and ¹H₃CO nuclei differ by a factor of 50 ($J_{PH} = 635$ vs 12 Hz), we assume scalar coupling of the electron to ¹H₃CO to be the weaker interaction as well.

Relaxation enhancements of the three MEP ¹H NMR resonances did not correlate with their J_{PH} coupling constants. Relaxation enhancements of the two types of methyl groups were similar despite the fact that their J_{PH} values differed by a factor of 10 (for POCH₃ and POCH₂CH₃, $J_{PH} = 11$ and ~ 1 Hz, respectively). For comparison, the ethyl methylene (POCH₂–CH₃) hydrogen coupling is slightly weaker than the methyl ester protons ($J_{PH} = 7$ and 11 Hz) and is the most strongly affected. From these observations, we conclude that scalar interactions contribute little to the relaxation of the alkyl protons of the dialkyl phosphate.

A Criterion for Using ³¹P Relaxation Enhancements To Study Metal/Ligand Exchange Rates: Implications for Metalloprotein Reactivity Studies. A long-term goal of this research is to develop methods for studying the interactions of probes with Mn-containing metalloproteins. Since metalloprotein behavior cannot be studied at elevated temperatures, an alternate technique is needed to determine whether the ³¹P T_{2par} is in slow exchange. We have shown in this work that comparison of relaxation enhancements of the ¹H and ³¹P nuclei of MeOPH provides the necessary data for such a determination for low molecular weight metal complexes. This method, as summarized below, is readily applicable to high molecular weight Mn-containing metalloprotein systems.

If (as assumed earlier) $\Delta\omega_M$ is negligible, line broadening of each of the NMR active nuclei of MeOPH will be determined by how its characteristic T_{2M} compares to τ_M (eq 3). The ³¹P nucleus is in slow exchange when $T_{2M,P}/\tau_M \ll 1$. Since all of the nuclei share the same τ_{sol} , line broadenings of the ¹H and ³¹P resonances ($\Delta\nu_H$ and $\Delta\nu_P$, respectively) can be used to relate their respective T_{2M} values ($T_{2M,H}$ and $T_{2M,P}$) to the shared τ_M . If the ratio $T_{2M,P}/T_{2M,H}$ can be estimated, then we can estimate how the relaxation times compare to the lifetime of the complex, eq 9.

$$T_{2M,P}/\tau_M = (\Delta\nu_P - \Delta\nu_H)/(\Delta\nu_H(T_{2M,H}/T_{2M,P}) - \Delta\nu_P) \quad (9)$$

If the slow-exchange threshold is presumed to occur where $T_{2M,P}/\tau_M \approx 5$, the criterion can be expressed as eq 10:

$$(\Delta\nu_P - \Delta\nu_H)/(\Delta\nu_H(T_{2M,H}/T_{2M,P}) - \Delta\nu_P) < 0.2 \quad (10)$$

This can only occur if the $\Delta\nu_P$ term in the denominator is negligible and eq 10 is approximately

$$(T_{2M,P}/T_{2M,H})(\Delta\nu_P/\Delta\nu_H - 1) < 0.2 \quad (11)$$

For cases where T_{2M} of both the ³¹P and ¹H–P nuclei are dominated by the scalar mechanism, relaxation is governed by A_{iso} and eq 12 holds.

$$T_{2M,P}/T_{2M,H} = (A_{iso,P}/A_{iso,H})^2 \quad (12)$$

If the ratio of the two isotropic coupling constants is equal to the ratio of the values in Table 3, the condition for slow exchange of the ³¹P nucleus can be reduced to eq 13.

$$\Delta\nu_P/\Delta\nu_{HP} < 11 \quad (13)$$

While eq 11 can be applied to unknown systems (such as metalloproteins), the criterion expressed in eq 13 should be used

(41) (a) Yordanov, N. D.; Zdravkova, M. *Chem. Phys. Lett.* **1986**, *127*, 487–491. (b) Buy, C.; Girault, G.; Zimmerman, J. L. *Biochemistry* **1996**, *35*, 9880–9891. (c) Halkides, C. J.; Farrar, C. T.; Larsen, R. G.; Redfield, A. G.; Singel, D. J. *Biochemistry* **1994**, *33*, 4019–4035.

(42) While $\Delta\omega_M$ is also field strength dependent, the effect we observe is more consistent with T_{2M} being modulated by τ_c ; if only τ_M and $\Delta\omega_M$ were important then T_{2par} should approach τ_{sol} (equal to the ³¹P T_2) as the square of the applied field.

with more caution. If the ratio $A_{\text{iso,P}}/A_{\text{iso,H}}$ is significantly different than reported here, or if dipolar terms contribute significantly to relaxation, then eq 13 will not hold. It is especially important that dipolar terms are not neglected when studying macromolecules. When molecular tumbling rates are slow, dipolar relaxation by the Curie mechanism may be an important factor. When both dipolar and scalar interactions are important, a more involved method will be required to estimate $T_{2M,P}/T_{2M,H}$ for use in eq 11. Suggested methods for determining when dipolar relaxation is important and for estimating $T_{2M,P}/T_{2M,H}$ under these conditions are included in the Supporting Information section of this paper.

Conclusions

The data contained herein support a model where the ^{31}P T_{2M} values for complexes formed between each of the two probes (MeOPH and MEP) and each of the two metal complexes ($\text{Mn}(\text{H}_2\text{O})_6^{2+}$ and $\text{Mn}^{\text{III}}\text{TMPyP}^{5+}$) are short compared with the mean lifetimes (τ_M) of the metal/probe complexes. T_2 relaxations of the ^{31}P resonances of each of the probes and that of the ^1H -P resonance of MeOPH are governed by scalar interaction with the metal ion. In contrast, relaxation of alkyl hydrogen nuclei

occurs by a dipolar mechanism. Consistent with our EPR and variable temperature NMR studies, we propose that the R_{2P} of the MeOPH ^{31}P resonance is equal to the second-order rate constant for ligand exchange when eq 11 is satisfied. This result indicates that chemical kinetics can be determined for paramagnetic metal complexes for systems where variable temperature studies are impractical. From these results, we conclude that MeOPH and MEP are suitable probes for measuring reactivities of paramagnetic metal sites in metal complexes, including metalloproteins and other catalytically active molecules.

Acknowledgment. The authors are grateful to Dr. David W. Randall (UC Davis) for programming the ENDOR simulation routine and are grateful for financial support from NIH grants GM61211-01 (UC Davis) and 1 R21 RR14018-01 (Duke).

Supporting Information Available: Data from individual experiments and a discussion of approximations and assumptions made in the analysis. This material is available free of charge via the Internet at <http://pubs.acs.org>.

IC010728W